Nanomedicine Formulations for Respiratory Infections by Inhalation Delivery - Covid-19 and Beyond

Preprint · March 2020

DOI: 10.31219/osf.io/adnyb

1 author:

Oron Zachar
Biovo Technologies Ltd.
42 PUBLICATIONS **1,162** CITATIONS

SEE PROFILE

Article

Nanomedicine Formulations for Respiratory Infections by Inhalation Delivery: Covid-19 and Beyond

Oron Zachar [1*]

[1] Yamor Technologies Ltd
* Correspondence: oronz@vytonic.com

Abstract: We present novel candidate formulations and realistic delivery dosages for a broad-range antiviral and antibacterial treatment based on nanoparticle colloids (NpC) delivered by inhalation. We lay the groundwork for clinical evaluation of this treatment by analysis of formulation composition, dosage calculation, delivery method, and clinical safety. Our core calculations are phenomenological and independent of microbiological mechanisms of action. Nevertheless, we propose possible mechanisms to guide future optimization and alternatives. Specifically, many viruses have dominant positively-charged spike protein sections, whereas NpC have a large negative zeta-potential. Hence, electrostatic binding of the nanoparticles to virus spikes neutralizes their binding affinity to host cell receptors. Our results suggest that any NpC with nanoparticle diameter 2–10 nm and a large negative zeta-potential will be effective against viruses with predominantly positively-charged spike proteins, but ineffective against viruses with predominantly negatively-charged spike proteins. Comparing the effective inhibitory concentration (IC) required in the target airway surface liquid (ASL) with the established safety range for such nanoparticles by inhalation intake, we conclude that there is a very wide range of safe and effective dosages that can be clinically explored. We suggest that inhalation delivery of the proposed antiviral formulations should be applied as a first-line intervention while respiratory infections are primarily localized to the upper respiratory system and bronchial tree. We note that similar NpC dosages also provide antibacterial effectiveness and therefore propose that inhalation delivery of NpC be implemented prophylactically in intensive care units to lower the risk of hospital ventilator-associated pneumonia (VAP).

Keywords: nanoparticles; nanomedicine; respiratory infections; silver; virus; VAP; colloid; SARS-CoV-2; Covid-19, influenza

1. Introduction

The antibacterial and antiviral potential of nanoparticle colloids (NpC) has been extensively demonstrated in in-vitro and animal testing [1–6]. Medical anti-microbial applications of NpC for wound care is approved by the FDA. Unfortunately, a senseless and uncontrolled "alternative medicine" practice of silver NpC ingestion led the pharmacological and academic establishment to widely disregard the potential application of metal-based NpC as antimicrobial agents in contexts other than wound care. In particular, there has been no rigorous analysis of the potential use of inhalation-delivered NpC for the prevention and/or treatment of respiratory infections.

In this article, we analytically substantiate the potential of antimicrobial NpC formulations, delivered by inhalation, to minimize the aggravation of respiratory system infections. We evaluate both (A) viral respiratory infections (including with SARS-CoV-2, the causative agent of COVID-19), and (B) bacterial infections, particularly ventilator-associated pneumonia (VAP) in intensive care unit

(ICU) patients. Indeed, the most reliable experience concerning the treatment of respiratory infections has been gained in the context ICU-acquired VAP, for which it is recognized that aerosolized antimicrobials represent an attractive alternative treatment modality that possesses numerous potential advantages over oral or intravenous antibiotics [7]. However, there are several unique factors to consider for optimal treatment of the lungs. These include aerosol characteristics, breathing patterns, geometrical factors (lung morphology), disease state, pharmacokinetics (including lung clearance and mucus transport). Aerosol characteristics are mainly determined by inhalation device. Not only the total pulmonary drug dose, but also the regional deposition distribution of the lung-deposited aerosol is a key factor for the clinical success of an inhalation therapy [8].

Commonly, the pathogenesis of respiratory infections begins mildly in the nasopharynx and/or upper bronchial tree portions of the respiratory system [9,10]. Aggravation occurs once the pathogens and associated inflammation migrate to lower portions of the respiratory system. Moreover, as the infection spreads, increased immune response may exacerbate the clinical condition [11]. Greater risk together with aggravation of the disease state is characterized by increased microbial load in the upper bronchial tree. Hence, a desirable clinical endpoint for the proposed inhaled NpC treatment is inhibition of microbial load in the upper sections of the bronchial tree, thereby lowering the risk of infection aggravation and spread. Such an endpoint implies treatment when most patients are still at home with mild symptoms, or in hospital ICU and from day-one of patient admission, as a prophylactic treatment before signs of any VAP infection emerge.

To the best of our knowledge, no theoretical or clinical research on the medicinal inhalation of silver-based NpC has been published. In this article, we intend to lay the groundwork for future clinical evaluations of inhaled NpC by determining: (i) the NpC material composition required for effective antiviral activity; (ii) the effective inhibitory concentration (IC) required in target respiratory tissues; and (iii) the dosage required for practical inhalation delivery of metal-based NpC antiviral and antibacterial formulations.

2. Materials and Methods

Guided by the discussion of Hasan and Lange [12], we adapt the core principles of antibiotics inhalation delivery in the context of ventilated ICU patients [7] to aerosol delivery of antimicrobial doses to non-ventilated patients, as illustrated in Figure 1.

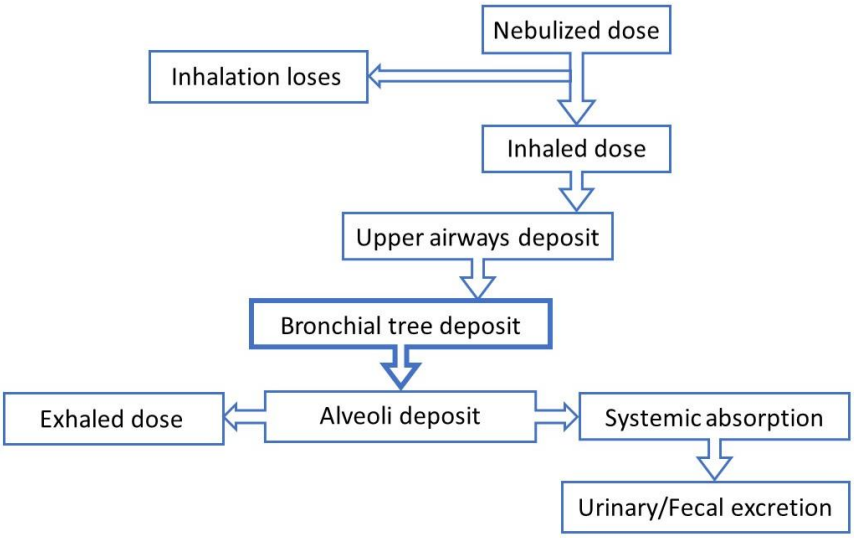

Figure 1. Mechanisms by which the dose of an antimicrobial agent inserted into a nebulizer differs from the dose delivered to the target airway location (based on [7]), with a focus on the fraction deposited in the bronchial tree.

As elaborated below, our dose calculation is derived from the following analytical results:

- Nanoparticles: For antiviral applications, nanoparticle size should optimally be in the range of 3–7 nm. In manufacturing, the stabilizing ("capping") agent used is significant. It appears that polymer capping agents (PVP, PVA) reduce the antiviral effectiveness of NpC. For antibacterial applications, there is less sensitivity to nanoparticle size and stabilizing method.
- Target inhibitory concentration (IC): For antiviral applications, effective target IC is about 10 μg/mL for silver nanoparticles. Higher dosages, of around 20 μg/mL, are needed for antibacterial applications.
- Tissue deposition fraction (TDF): During oral breathing of 5 μm aerosol droplets, NpC deposit onto the pharynx (30%), bronchial tree (30%), and alveoli (25%).
- Inhalation time losses (ITL): inhalation duration is about a third of the breathing cycle. Thus, using a continuous aerosol source, only about 30% of the nebulized substance is actually inhaled.

To calculate the required delivery dose, we implemented a stepped procedure, evaluating the effect of each stage between the aerosol produced by the aerosolizing device and final target tissue deposition. Equation 1 delineates the required NaC aerosolized dose (AD) calculation:

$$AD = \frac{IC \times MV}{TDF \times ITL \times CC} \quad (1)$$

where AD (mg) is a function of the target inhibitory concentration (IC, μg/mL), mucosal volume (MV, mL), tissue deposition fraction (TDF), inhalation time losses (ITL), and colloid concentration (CC, μg/mL).

3. Results

Table 1 summarizes a possible antiviral formulation for the oral inhalation of 5 μm aerosol droplets, as calculated from Equation 1. Using a continuous nebulizer, a nebulized dose of 3.3 mL is required to effectively deposit the IC in the bronchial tree. Nebulizing 3ml to 6 mL of drug solution for inhalation delivery (assuming 10–20% effective lung deposition) is a common practice in hospital ICUs [13]. Hence, we similarly expect inhalation of 3ml to 6 mL nebulized dose to be well-tolerated. We note that, because the mucosal volume in the bronchial tree is about ten times greater than that found in the alveoli, targeting the IC to the alveoli requires a significantly higher concentration of silver NpC source. Since smaller droplets are more preferentially deposited in the alveoli, it may be recommended to use a 3 nm-droplet aerosol when targeting the alveoli (Table 1).

Table 1. Dose calculations for aerosol droplets of various sizes to treat different target tissues

Target tissue	Droplet size (μm)	IC required at target tissue (μg/mL)	Mucosal volume (mL)	Deposition fraction	Colloid concentration (μg/mL)	Inhaled dose (mL)	Continuous nebulized dose (mL)
Bronchial tree	5	10	1	0.3	30	1.1	3.3
Bronchial tree	3	33	1	0.1	150	2.2	6.6
Alveoli	3	10	10	0.3	150	2.2	6.6

On the basis of prior experience with established antibiotic inhalation treatments, a practical inhaled antimicrobial dose should be some significant multiple of the theoretical doses above, and may be verified by in vivo sampling (e.g., using BAL sampling in ventilated patients). Hence, in practice it may be that doses three times greater than the above are needed to achieve effective IC.

3.1. Target IC Determination for Antiviral Applications

In the context of inhalations, the relevant configuration is nanoparticles suspended in aqueous media. The key starting point for calculating any effective dose is to establish the required target IC of the effective agent. Antiviral effect is obtained only by nanoparticle sizes of <10 nm (as discussed in section 3.2 below). The capping molecule used during nanoparticle manufacture to achieve size stabilization affects antiviral potency. The popular PVP cap appears to significantly inhibits antiviral effectiveness. Therefore, in analyzing the published data, we limit our consideration to experiments involving nanoparticles of size <15 nm and to non-PVP-stabilized NpC. The evidence summarized in Table 3 indicates that an IC of at least 10 μg/mL is desirable at the target respiratory system location. We note that one of the referenced experiments was conducted on a coronavirus. **Our analysis suggests that the optimal size of silver nanoparticles for antiviral effectiveness is in the range of 3–7 nm, not the 10 nm diameter used in all the referenced experiments. Hence, there is potential for even better efficacy and/or lower dose if an optimal NpC diameter is used**. In the published experiments (Table 2), it is likely that all the antiviral effectiveness arises from the margins of the particle size distribution range, within the noted range of <10 nm.

Table 2. Target inhibitory concentration (IC) for non-PVP stabilized nanoparticle colloids (NpC) with diameter ≤10 nm

Virus	NpC diameter distribution peak (nm)	IC (μg/mL)	Reference
Influenza A H3N2	9.5	<12.5	[14]
Monkeypox (MPV)	10	<12.5	[15]
Coronavirus TGEV [1]	10	~10	[16]
Tacaribe (TCRV)	10	<10	[17]

[1] TGEV, transmissible gastroenteritis virus

3.2 Relation to the Mechanism of Action

Our core calculations are phenomenological and thus are not dependent on mechanisms, yet an understanding of mechanisms may guide future treatment optimization and alternatives. We should distinguish between the mechanisms of NpC action on bacteria and viruses. There appear to be a multitude of possible ways for bacteria to interact with silver NpC components (both the nanoparticles and Ag^+ ions), which have been suggested and discussed by others [18]. In contrast, on the basis of the broad-range effectiveness of silver NpC with diverse capping surface molecules against many different viruses, we shall argue that the underlying mechanism of action of NpC must be non-specific, simple, and robust. In particular, we argue below that the silver is not important in itself other than as a manufacturing basis for nanoparticles with appropriate physical properties. The prominant material properties of the colloid that affect its antiviral binding action are the physical nanoparticle size and surface zeta potential, with all remaining aspects of the chemical composition being secondary. Hence, other NpC with these properties, such as NpC based on metal-oxides (e.g., zinc oxides, titanium oxides) would be effective as well.

3.2.1 Antiviral Mechanism of Action – Nanoparticle Size

The importance of nanoparticle size is much greater for antiviral compared with antibacterial properties. We contend that this is related to the mechanism of action. Unlike bacteria, against which both dissolved silver ions (Ag^+) and nanoparticles appear to have an effect, the antiviral effect arises

predominantly from attachment of the nanoparticles themselves to the virus. We posit that there is an essential universality to antiviral effectiveness being limited to nanoparticle sizes of <10 nm, with this universality arising from the roughly uniform geometric scales of respiratory infection viruses (e.g., influenza and coronavirus): having diameters of about 100 nm, the distance between neighboring spike glycoproteins being 10–20 nm, and the glycoprotein characteristic length being about 15 nm. Thus, based on geometrical limitations alone, for a nanoparticle to interact effectively with a glycoprotein site, its diameter must be on the order of 10 nm or less. Virus functioning becomes disturbed only when the virus is sufficiently covered by attached nanoparticles [19].

We find supporting evidence for the above argument from experiments and direct imaging of nanoparticles binding to human immunodeficiency virus (HIV) [20], whose size is 120 nm, with ~22 nm spacing between the glycoprotein knobs. Interestingly, the observed sizes of nanoparticles bound to HIV (see Figure 2) are exclusively within the range of 1–10 nm, with peak virus attachment effectiveness for nanoparticle sizes in the range of 3–7 nm. No nanoparticles with diameter >10 nm were observed to interact with the virus, which is noteworthy, given that ~40% of the overall nanoparticle population in the sample was beyond this size range [20].

Consequently, we estimate that experiments in the literature, performed with larger NpC, have skewed target IC values too high, since their effectiveness arises wholly from the margins of the distribution of particles with sizes <10 nm. Hence, we focused on analyzing published data from experiments conducted with ~10 nm NpC size.

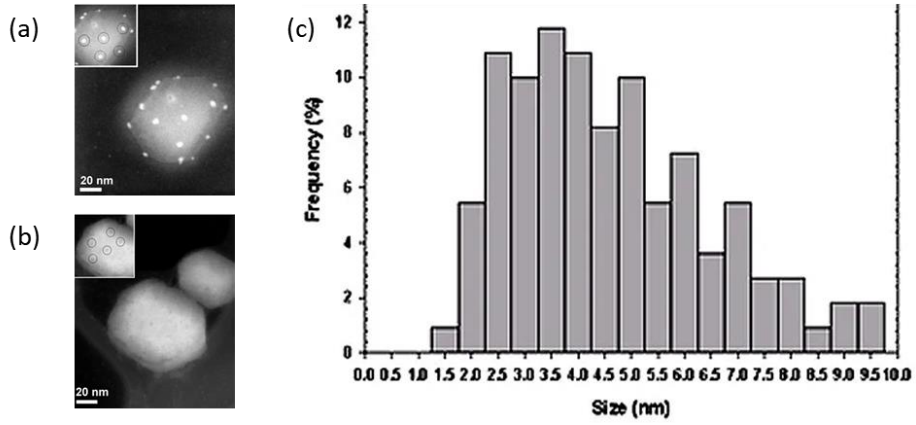

Figure 2. HIV-1 (**a**) with and (**b**) without silver nanoparticle treatment. (**c**) Composite size distribution of silver nanoparticles bound to HIV-1 derived from all tested preparations seems to peak at a nanoparticle size of about 4 nm (adapted from [20]).

3.2.2 Antiviral Mechanism of Action –The Electrostatic Potential of Nanoparticles

Nanoparticles are composites, having a metal core and an envelope capping material (Fig. 3). In a liquid environment, nanoparticles have a surface electric potential, called the zeta potential, that is dependent on environmental pH. For a typical silver NpC, the zeta potential is negative.

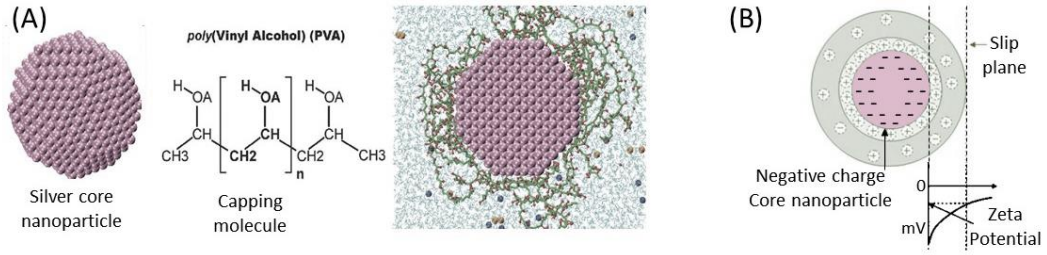

Figure 3. (**a**) A silver nanocrystal core, the PVA capping, and a full snapshot of an equilibrated PVA-stabilized nanoparticle in aqueous media [21]. (**b**) The zeta potential of a colloidal nanoparticle is the potential (here negative) at the slip plane surface.

Unlike bacteria, we conjecture that the broad-range antiviral effectiveness of NpC is a consequence of the purely electrostatic nature of the interaction. The spike proteins of many viruses (including influenza and coronaviruses) are positively charged, likely promoting their binding to the predominantly negative surface charge of the host cell receptors (such as ACE2) [22]. Correspondingly, the highly negative surface zeta-potential of the nanoparticles (which is required to keep them in colloidal form) leads the nanoparticles to bind selectively to the spike proteins of viruses and thereby neutralize their receptor binding affinity. Hence, nanoparticles with a zeta potential stronger than -20 mV or -30 mV are preferred. This also explains why the positively charged silver ions play a negligible role. The silver as a particular atom is unimportant in itself, other than as a manufacturing method for generating a stable, charged, composite nanoparticle colloid. It follows that any colloid of nanoparticles whose size distribution is predominantly in the 2–10 nm range and that possess a highly negative zeta-potential of strength more than -20 mV would work as effectively as silver NpC. Correspondingly, we conjecture that viruses whose spike protein binding sites are less positively charged will be less affected by the standard silver NpC with negative zeta potential.

Generally, the zeta potential becomes more negative with increasing pH. Plotting the range of values for the zeta potential with changing pH produces a titration curve of pH vs. zeta potential. The pH at which the zeta potential crosses between negative and positive values is called the isoelectric point. In humans, normal pH values of tracheal mucus are in the range 6.9–9.0 [23]. Therefore, NpC preferably should have a pH of around 7–7.5 in order that their zeta potential not overly degrade in the biological mucosal environment.

3.3 Coronavirus Evidence

Transmissible gastroenteritis virus (TGEV), a porcine coronavirus, causes very high mortality in piglets. Vaccination has been extensively applied to prevent TGEV infection in pigs, however, the resulting immune efficacy appears to be less than ideal and the potential for dissemination as well as prevalence of the infectious agent in piglets remains [16]. Figure 4 presents the results of testing the effect of NpC on coronavirus TGEV [16]. With nanoparticles of non-optimal size 10–20 nm there is a significant effect at a concentration of 12.5 μg/mL.

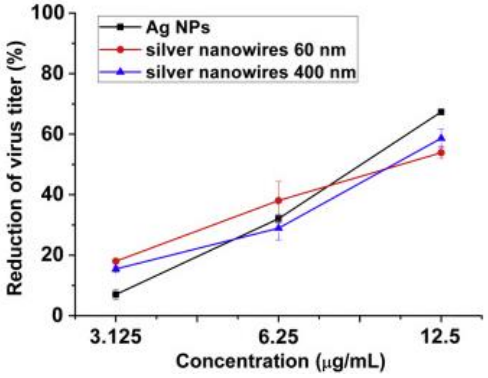

Figure 4. The coronavirus TGEV (MOI 0.5) was incubated with the indicated concentrations of AgNP at 37 °C for 1 h in DMEM. The indicated AgNP are nanoparticles of size <20 nm (adapted from [16]). AgNP, silver-based nanoparticles.

3.4 Distinguishing Ionic vs Nanoparticle colloids

It is important to distinguish between ionic solution (recognized by clear water-like color) and *nanoparticle colloids* (recognized by a visibly brownish color). For example, with Silver, ionic silver solution consists of silver ions dissolved in water, whereas silver NpC consist of nano-sized chunks of elemental silver, with diameters of 1–100 nm. With respect to *antibacterial* properties, both ionic silver and silver NpC are effective agents. In contrast, regarding *antiviral* properties, it has been argued that colloidal particles are about 10 times more potent than ionic silver [24].

3.5 Significance of Selected Stabilization Coating of the Nanoparticles

There are indications in the literature that the capping agent material can affect antiviral effectiveness. For example, it appears that PVP-capped NpC had practically no antiviral effect on the coronavirus TGEV, whereas a non-PVP NpC exhibited strong antiviral effectiveness [16]. A similar result was obtained for HIV, where a ten-fold greater concentration was needed for a PVP-coated NpC sample to achieve the same antiviral effect as a non-PVP NpC [20]. Overall, it appears that a thinner capping layer may have a less deleterious effect on antiviral potentcy.

3.6 Target inhibitory concentration (IC) Determination for Anti-bacterial Applications

For bacterial infections, the literature suggests the presence of a poorly differentiated mixed effect arising from both silver ions and nanoparticles. A major problem in deriving clear numerical conclusions from the published literature is that the IC, stated in weight fraction units (μg/mL), is very sensitive to nanoparticle size. For the same weight fraction (μg/mL), the required IC will be lower for smaller nanoparticles compared with larger nanoparticles, which is indeed the case experimentally [25]. To understand it, we note that for the same weight fraction (μg/mL) there would be a higher numerical density of smaller nanoparticles than larger nanoparticles (nanoparticle number density is roughly proportional to $1/R^3$, where R is the particle diameter). Since higher number density increases the probability of nanoparticle–pathogen interactions, we would expect smaller nanoparticles to exhibit greater antimicrobial effectiveness than larger nanoparticles. Since different published studies used different sized nanoparticles, the resulting IC values vary significantly between publications as **an artifact of the different nanoparticle sizes used in the various protocols, thereby obscuring and confusing variability in NpC effects**. The particular concentration kill dependence is not well researched. Specifically, in the antimicrobial dosing literature there are three major patterns of antimicrobial kill characteristics: (i) "concentration-dependent killing", determined by the maximal concentration (Cmax); (ii) "time dependent killing", determined by exposure time at concentrations greater than the minimal inhibitory concentration (MIC); and (iii) area under the concentration–time curve (AUC), determined by AUC at concentrations above MIC. However, there is no clear analysis of these aspects in the published literature, to the best of our knowledge.

Considering the antibacterial properties of silver NpC against at least some clinically important bacteria (such as Pseudomonas aeruginosa) [25], it still appears that the typical IC values (~7 μg/mL) of small nanoparticles (~7 nm) are similar to those of the typical antiviral IC, according to our above analysis. Therefore, NpC diameter <10 nm is also optimal for antibacterial applications, and a similar IC target concentration of ~10 μg/mL is expected to be effective for both antiviral and antibacterial respiratory infection treatment applications.

3.7 Dose Calculation

Antimicrobial drugs exhibit concentration-dependent efficacy. Therefore, ensuring an appropriate concentration of these drugs in the relevant body fluid is important for obtaining the desired therapeutic action. For inhaled antimicrobials, the relevant body fluid for drug concentration purposes is the airway surface liquid (ASL) [12], also referred to as epithelial lining fluid (ELF). The delivered dose is deposited on and diluted by the ASL. We argue that dosage planning, correction, and controlled verification can all be achieved by focusing on and examining the trachea and/or primary bronchi (first generation, G1). Deposition models suggest that the trachea can serve as a good concentration estimator (to within a factor of three) and effective lower bound for all of the first 10 generations of the bronchial tree, as illustrated in Fig. 5. Therefore, tracheal concentration is an effective, well-defined, and measurable representative of target IC.

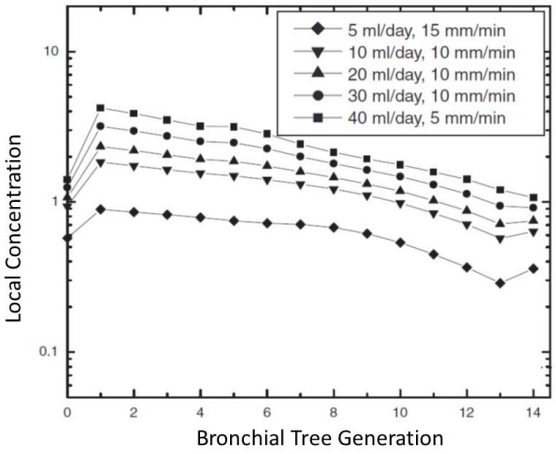

Figure 5: Local concentration of inhaled aerosol in different generations of the bronchial tree, where the trachea is generation 0. Adapted from [12].

Theoretically, calculating the intake dosage that needs to be deposited to achieve the target IC requires knowing the volume of the ASL. However, unlike the predictability of blood volume (for IV delivery), the ASL drug concentration resulting from aerosol inhalation deposition has significant inter-personal variability. Such variability may result from individual disease states (e.g., pneumonia, cystic fibrosis, healthy) or lifestyles (e.g., smoking). Verification of the ASL concentration per individual can be achieved from direct measurement of bronchoalveolar lavage (BAL) samples.

3.7.1 Concentration in Airway Surface Liquid (ASL)

A dose calculation yields a range of possibilities, rather than a fixed number. Several aspects and considerations should be taken into account. Two important concepts are the minimum inhibitory concentration (MIC) and the target IC. In clinical practice, the indicated dosage is expected to be a significant multiple of the MIC within wide clinician-determined margins limited by the bounds of safety. It is quite common for inhalation antibiotics to set a target IC that is even ten times (10x) the MIC. For our nanoparticle dose calculation, if the target MIC is 10 μg/mL, then the clinically desired antiviral effective IC in the ASL may be ten times greater (*i.e.*, 100 μg/mL).

The total surface area of the bronchial tree is about 1 m^2 (10,000 cm^2). Using the surface area and mucosal thickness data from Table 3, we estimate the combined mucosal volume in the top half of the bronchial tree to be about 1 mL in a healthy adult. The total surface area of the alveoli is about 100 m^2 (*i.e.*, 1,000,000 cm^2), with mucosal thickness of about 0.07 μm, resulting in a total ASL volume of 7–10 mL . Therefore, disinfection of the upper bronchial tree at early stages, before the infection has spread deep into the lungs, is the most reasonable and realistic target treatment.

298 **Table 3.** Surface area and mucosal thickness of various parts of the bronchial tree [1]

Generation (k) [2]	$th_{k, PLC}$ [3] (μm)	Airway surface area (cm^2)
0	6.04	70.83
1	5.49	32.11
2	5.02	40.10
3	4.61	50.74
4	4.27	63.17
5	3.99	63.96
6	3.74	81.88
7	3.53	121.20
8	3.36	171.36
9	3.21	228.98
10	3.08	289.24
11	2.97	353.44
12	2.88	422.64
13	2.81	520.41
14	2.74	687.61

299 [1] Adapted from [12]; [2] Generation k = 0 is the trachea; $th_{k, PLC}$ is the thickness at generation k of
300 the periciliary layer.

301

302 A significant factor affecting inhalation antimicrobial delivery is the disease state. Increased
303 mucus production will dilute the drug concentration compared with the theoretical estimation above,
304 which is based on the lung mucosal volume data for healthy adults. The earlier the intervention,
305 before a significant increase in additional mucosal volume, the more predictable the effective dose.
306 Fortunately, for inhalation of NpC formulations, our theoretically computed MIC is more than 100
307 times smaller than any estimated safety limit in the regulatory literature. Hence, clinical research of
308 higher doses is possible.

309 3.7.2 Deposition Fraction in Target Tissue

310 The deposition fraction factor depends on the:

311 i. Target tissue location: extra-thoracic, in the trachea-bronchial (TB) tree, or
312 pulmonary (alveoli)
313 ii. Mode of inhalation: nasal or oral
314 iii. Size of the aerosol droplets.

As illustrated in the Fig. 6, there is a significant difference in tracheal-bronchial (TB) tree deposition between nasal and oral breathing. Peak nasal breathing TB deposition is only about 10%, whereas oral breathing TB deposition is about 30%. Hence, **we recommend oral inhalation**.

The dependence of deposition fraction on aerosol droplet size is also different in each tissue region. In order to achieve optimal utilization, or to facilitate more practical inhalation conditions, aerosol size should preferably correspond to peak probability of deposition in the target tissue. As illustrated in Fig. 6: (a) the peak bronchial tree deposition fraction (of ~30% or more) is obtained with aerosol droplets of diameter ~6 μm, whereas (b) peak alveoli deposition (of ~30% or more) is obtained with aerosol droplets of diameter ~3 μm. The droplet diameter achieved by many standard mass-produced devices presently on the market is about 5 μm on average, which is expected to be adequate for antimicrobial NpC treatment purposes. **For 5 μm droplets, the bronchial tree deposition fraction is ~30% and alveoli deposition fraction is ~25%.**

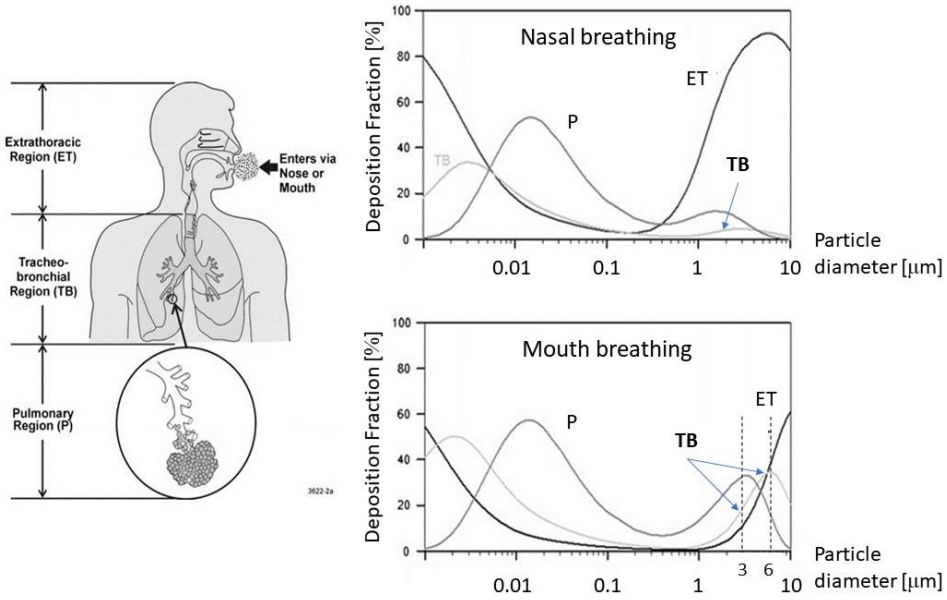

Figure 6. Primary structures of the respiratory system and associated nanoparticle deposition fractions when breathing at rest. Adapted from [26].

3.7.3 Inhalation Timing Losses

Inhalation represents only about a third of the duration of a full breathing cycle. Hence, when aerosols are delivered continuously, only about a third of the aerosolized dose is considered to have been delivered effectively. This would be the common situation for home users utilizing standard commercial medicament aerosol devices available for purchase in pharmacies. By contrast, using a breath-actuated nebulizer (also available commercially) would correspondingly avoid wastage of silver NcP colloid during the approximately two thirds of the breathing cycle that is not inhalation.

3.7.4 Lung Clearance

The lungs have innate mechanisms to remove deposited particles. Thus, we need to examine whether the nanoparticles reside long enough in respiratory system surface tissue to fulfil their antiviral potential. For indicative reference, we consider the behavior of inhaled antibiotics (tested in ventilated ICU patients) [27,28]. We note that inhalation-deposited antibiotics reside for an effective peak duration of about 2–3 h in the lungs. The NpC experimental data that we analyzed were commonly for 1 h treatments (e.g., for the coronavirus presented in Fig. 4). Hence, experience with inhaled antibiotics suggests that the proposed NpC inhalation will be retained in lung surface tissue for long enough to exhibit antiviral potency.

3.7.5 Clinical Safety

Clinical safety evaluations are performed in the context of an estimated treatment dose and schedule. According to Table 1, a minimal IC would require silver NpC treatment deposition of 11 μg, which can be obtained from the inhalation of about 33 μg of silver aerosol (since only about 30% of the inhaled dose is deposited). If treatment is performed three times daily, this translates to a daily deposition of about 33 μg and aerosol inhalation of 100 μg. Nevertheless, and as discussed above, experience with antibiotic inhalation leads us to assume that, in practice, achieving the inhalation IC requires significantly higher dosages than those derived from the in vitro evidence. For example, for the sake of analysis, we may assume a recommended IC dose of three times (3x) the above noted in-vitro dose, which amounts to a daily deposition of about 100 μg and aerosol inhalation of 300 μg, taken over a five-day period (similar to an antibiotics regimen).

People are exposed daily to silver via the intake of food and water. The human body has inherent mechanisms for the disposal of silver. The median daily intake of silver from food and drinks has been reported to be in the range of 20–80 μg/day [29]. Therefore, our above scenario of a recommended treatment regimen (deposition of about 100 μg) can be considered a moderate increase over normal daily dietary intake for a short acute treatment duration of a few days.

When addressing safety and/or toxicity, the professional guidelines distinguish between acute exposure of less than 14 days and prolonged (repeated dose) or chronic exposure of more than 14 days. In our context, only acute (<14 days) exposure is relevant, but we shall discuss both.

There are several occupational guidelines and exposure limits in the USA for airborne silver dust. All are defined on a mass basis. The Occupational Safety and Health Administration (OSHA) has adopted the value of the American Conference of Governmental Industrial Hygienists (ACGIH) for the threshold limit, being a threshold-limit value time-weighted average (TLV-TWA) chronic exposure over a 40-hr week of 100 μg/m^3 (0.1 μg/L) of metallic silver dust. Under normal breathing of 6–8 L/min, this corresponds to silver nanoparticle inhalation of 36–42 μg/h. For a safe work environment (eight hours per day), this equates to daily inhalation of ~300 μg of silver nanoparticles on a routine prolonged basis. We therefore proclaim that **the treatment regimen stipulated here of 300μg dose given three times daily lies within the safety bounds for acceptable chronic intake in the work environment in the USA**. However, chronic work environment exposure is not the appropriate context for a drug toxicity evaluation. We should look for evaluation and evidence regarding more short-term inhalation of silver nanoparticles.

In the context of inhalation delivery, it has been shown that even after 90 days of continuous inhalation exposure to high doses of silver nanoparticles (total of 1,143 μg/day of silver, *i.e.*, ten times (10x) the IC in Table 1, assuming treatment three times per day), the accumulated tissue levels recover to normal within about 12 weeks (see Figure 7). This provides a very strong indication of the safety of short-term inhalation exposure, in that it does not lead to lasting accumulation in body tissues.

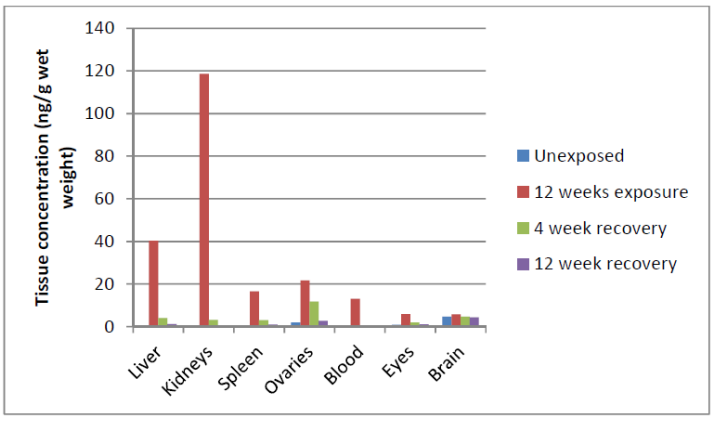

Figure 7. Tissue silver concentrations in female rats exposed to high levels of AgNP (381 μg/m^3 silver nanoparticles of ~15 nm diameter, for 6 h/day, which amounts to an inhalation dosage of 1,143 μg/day of silver) in a 90-day inhalation study, followed by a 12-week recovery period. Adapted from [30,31].

The test closest to our envisioned treatment protocol was performed on rats for 10 days, 4 hours/day, at a concentration of 3,300 μg/m^3 (3.3 μg/L) using an aerosol of 5 nm silver nanoparticles, and it resulted in minimal pulmonary toxicity or inflammation [32]. For a human breathing at a normal resting rate of 6 L/min, this translates to a daily inhaled dosage of silver nanoparticle aerosol of 4,700 μg/day. This study indicates that, for acute short-term treatment of less than 10 days, even an inhalation intake of 4,000 μg/day, which is about 100 times (100x) the IC dose in Table 1, would induce no adverse reaction.

4. Discussion

Though marred by the charlatan claims of unprofessional "alternative medicine" commercial products, there is well-established scientific research on the antibacterial and antiviral properties of silver NpC. Yet, its potential application for the treatment of respiratory infections has never been properly explored, to the best of our knowledge. The surveyed literature indicates that silver NpC of diameter 3–7 nm can be highly effective in suppressing viral infections. We further conclude that the IC concentration of such colloids is about 10 μg/mL (Table 1). However, we obtained these values by making somewhat indirect inferences and therefore more focused research is called for. In particular, for the treatment of lung infections via inhalation delivery (Table 1), a minimal IC would require silver nanoparticle treatment deposition of 11 μg, which can be obtained from the inhalation of about 33 μg of silver aerosol (since only about 30% of the inhaled dose is deposited). For treatment delivered three times daily, this corresponds to a daily deposition of about 33 μg and aerosol inhalation of 100 μg. However, experience with antibiotic inhalation leads us to assume that, in practice, inhalation IC will require substantially higher dosages that those derived from the in vitro evidence. For example, we estimate a recommended IC dosage of three times (3x) the in vitro dose, which amounts to daily deposition of about 100 μg and aerosol inhalation of 300 μg, taken over a 5 days period (similar to an antibiotics regimen). The available safety information indicates that such doses and regimens are well within the safe range and enable the safe delivery of even ten times (10x) the IC noted in Table 1. We estimate that these formulations can be effective for the prevention and treatment of any early-stage respiratory viral infection, including infection with SARS-CoV-2.

To set the scale of potential benefits, we flash out the remarkable results of an Influenza H3N2 in-vivo experiment done on mice by Xiang et al. (one of the very few in vivo animal experiments in the NpC literature), comparing the effectiveness of intranasal administration of NpC to that of Tamiflu (Oseltamivir) [27]. Tamiflu is claimed to reduce the number of patients who have serious complications from the flu, such as pneumonia (by 44%) or hospitalization (by 63%). A NpC treatment, if as effective as in the mice model, could cost less than 1/10 fraction of Tamiflu, with much less side effect risk, can be available essentially OTC (as the market availability of NpC already is), and easily manufactured locally at any country in the world. As shown in Fig.8 below, it appears that potentially NpC can be as effective as Tamiflu. But no investment in clinical human trials was ever done to investigate the possibility. We can only speculate that this is due to the lack of financial incentives for any conventional pharma company to make the required investment in development and regulatory procedures. One of the main goals of this paper is to motivate and guide the future clinical and regulatory development of NpC treatment formulations.

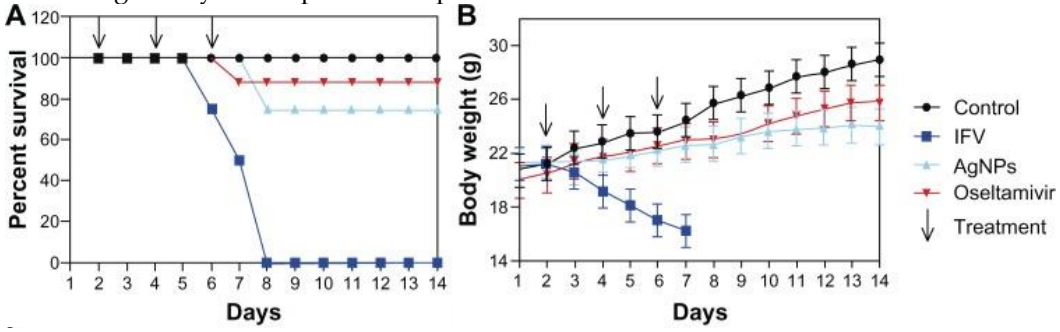

Figure-8: In-vivo intranasal NpC administration protected mice from H3N2 infection. (A) survival rate changes (%). (B) Changes in body weight (%). Adapted from [27].

For bacterial infections, particularly in the context of preventing ICU-acquired VAP, the same formulations are expected to be applicable. An additional risk-reduction benefit of silver NpC inhalation treatment for ventilated patients is the possibility of suppression of biofilm formation inside the endotracheal or tracheostomy tube.

Funding: This research received no external funding.

Acknowledgments: We thank Alex Singer for editorial assistance in the manuscript's preparation.

Conflicts of Interest: Yamor Technologies promotes a drug development program based on the framework presented in this article.

References

1. Aderibigbe, B.A. Metal-based nanoparticles for the treatment of infectious diseases. *Molecules* **2017**, *22*, 1370, doi:10.3390/molecules22081370.
2. Nakamura, S.; Sato, M.; Sato, Y.; Ando, N.; Takayama, T.; Fujita, M.; Ishihara, M. Synthesis and application of silver nanoparticles (Ag NPs) for the prevention of infection in healthcare workers. *Int. J. Mol. Sci.* **2019**, *20*, 3620, doi:10.3390/ijms20153620.
3. Siadati, S.A.; Afzali, M.; Sayadi, M. Could silver nano-particles control the 2019-nCoV virus?; An urgent glance to the past. *Chem. Rev. Lett.* **2020**, *3*, 9–11, doi:10.22034/crl.2020.224649.1044.
4. Galdiero, S.; Falanga, A.; Vitiello, M.; Cantisani, M.; Marra, V.; Galdiero, M. Silver nanoparticles as potential antiviral agents. *Molecules* **2011**, *16*, 8894–8918, doi:10.3390/molecules16108894.
5. Balavandy, S.K.; Shameli, K.; Biak, D.R.B.A.; Abidin, Z.Z. Stirring time effect of silver nanoparticles prepared in glutathione mediated by green method. *Chem. Cent. J.* **2014**, *8*, 11, doi:10.1186/1752-153X-8-11.
6. Haggag, E.; Elshamy, A.; Rabeh, M.; Gabr, N.; Salem, M.; Youssif, K.; Samir, A.; Bin Muhsinah, A.; Alsayari, A.; Abdelmohsen, U.R. Antiviral potential of green synthesized silver nanoparticles of Lampranthus coccineus and Malephora lutea. *Int. J. Nanomedicine* **2019**, *Volume 14*, 6217–6229, doi:10.2147/IJN.S214171.
7. Rouby, J.J.; Bouhemad, B.; Monsel, A.; Brisson, H.; Arbelot, C.; Lu, Q. Aerosolized antibiotics for ventilator-associated pneumonia: Lessons from experimental studies. *Anesthesiology* **2012**, *117*, 1364–1380, doi:10.1097/ALN.0b013e3182755d7a.
8. Darquenne, C.; Fleming, J.S.; Katz, I.; Martin, A.R.; Schroeter, J.; Usmani, O.S.; Venegas, J.; Schmid, O. Bridging the gap between science and clinical efficacy: Physiology, imaging, and modeling of aerosols in the lung. *J. Aerosol Med. Pulm. Drug Deliv.* **2016**, *29*, 107–126, doi:10.1089/jamp.2015.1270.
9. Behrens, G.; Stoll, M. Pathogenesis and immunology. In *Influenza Report*; Kamps, B.S., Hoffmann, C., Preiser, W., Eds.; Flying Publisher: Paris, France, 2006; pp. 92–109.
10. Garland, J.S. Ventilator-associated pneumonia in neonates: An update. *Neoreviews* **2014**, *15*, e225–e235, doi:10.1542/neo.15-6-e225.
11. Manjarrez-Zavala, E.M.; Patricia, D.; Horacio, L.; Ocadiz-Delgado, R.; Cabello-Gutierrez, C. Pathogenesis of viral respiratory infection. In *Respiratory Disease and Infection - A New Insight*; Mahboub, B.H., Ed.; InTech, 2013.
12. Hasan, M.A.; Lange, C.F. Estimating in vivo airway surface liquid concentration in trials of inhaled antibiotics. *J. Aerosol Med.* **2007**, *20*, 282–293, doi:10.1089/jam.2007.0603.
13. Dugernier, J.; Reychler, G.; Wittebole, X.; Roeseler, J.; Depoortere, V.; Sottiaux, T.; Michotte, J.B.;

Vanbever, R.; Dugernier, T.; Goffette, P.; et al. Aerosol delivery with two ventilation modes during mechanical ventilation: a randomized study. *Ann. Intensive Care* **2016**, *6*, 73, doi:10.1186/s13613-016-0169-x.

14. Xiang, D.; Zheng, C.; Zheng, Y.; Li, X.; Yin, J.; O' Conner, M.; Marappan, M.; Miao, Y.; Xiang, B.; Duan, W.; et al. Inhibition of A/Human/Hubei/3/2005 (H3N2) influenza virus infection by silver nanoparticles in vitro and in vivo. *Int. J. Nanomedicine* **2013**, *8*, 4103, doi:10.2147/ijn.s53622.
15. Rogers, J. V.; Parkinson, C. V.; Choi, Y.W.; Speshock, J.L.; Hussain, S.M. A preliminary assessment of silver nanoparticle inhibition of Monkeypox virus plaque formation. *Nanoscale Res. Lett.* **2008**, *3*, 129–133, doi:10.1007/s11671-008-9128-2.
16. Lv, X.; Wang, P.; Bai, R.; Cong, Y.; Suo, S.; Ren, X.; Chen, C. Inhibitory effect of silver nanomaterials on transmissible virus-induced host cell infections. *Biomaterials* **2014**, *35*, 4195–4203, doi:10.1016/j.biomaterials.2014.01.054.
17. Speshock, J.L.; Murdock, R.C.; Braydich-Stolle, L.K.; Schrand, A.M.; Hussain, S.M. Interaction of silver nanoparticles with Tacaribe virus. *J. Nanobiotechnology* **2010**, *8*, 19, doi:10.1186/1477-3155-8-19.
18. Dakal, T.C.; Kumar, A.; Majumdar, R.S.; Yadav, V. Mechanistic basis of antimicrobial actions of silver nanoparticles. *Front. Microbiol.* **2016**, *7*, 1831, doi:10.3389/fmicb.2016.01831.
19. Morris, D.; Ansar, M.; Speshock, J.; Ivanciuc, T.; Qu, Y.; Casola, A.; Garofalo, R. Antiviral and immunomodulatory activity of silver nanoparticles in experimental rsv infection. *Viruses* **2019**, *11*, doi:10.3390/v11080732.
20. Elechiguerra, J.L.; Burt, J.L.; Morones, J.R.; Camacho-Bragado, A.; Gao, X.; Lara, H.H.; Yacaman, M.J. Interaction of silver nanoparticles with HIV-1. *J. Nanobiotechnology* **2005**, *3*, 6, doi:10.1186/1477-3155-3-6.
21. Kyrychenko, A.; Pasko, D.A.; Kalugin, O.N. Poly(vinyl alcohol) as a water protecting agent for silver nanoparticles: The role of polymer size and structure. *Phys. Chem. Chem. Phys.* **2017**, *19*, 8742–8756, doi:10.1039/c6cp05562a.
22. Prabakaran, P.; Xiao, X.; Dimitrov, D.S. A model of the ACE2 structure and function as a SARS-CoV receptor. *Biochem. Biophys. Res. Commun.* **2004**, *314*, 235–241, doi:10.1016/j.bbrc.2003.12.081.
23. Clary-Meinesz, C.; Mouroux, J.; Cosson, J.; Huitorel, P.; Blaive, B. Influence of external pH on ciliary beat frequency in human bronchi and bronchioles. *Eur. Respir. J.* **1998**, *11*, 330–333.
24. Lara, H.H.; Ayala-Nuñez, N. V.; Ixtepan-Turrent, L.; Rodriguez-Padilla, C. Mode of antiviral action of silver nanoparticles against HIV-1. *J. Nanobiotechnology* **2010**, *8*, 1, doi:10.1186/1477-3155-8-1.
25. Martínez-Castañón, G.A.; Niño-Martínez, N.; Martínez-Gutierrez, F.; Martínez-Mendoza, J.R.; Ruiz, F. Synthesis and antibacterial activity of silver nanoparticles with different sizes. *J. Nanoparticle Res.* **2008**, *10*, 1343–1348, doi:10.1007/s11051-008-9428-6.
26. Cheng, Y.S. Mechanisms of pharmaceutical aerosol deposition in the respiratory tract. *AAPS PharmSciTech* **2014**, *15*, 630–640, doi:10.1208/s12249-014-0092-0.
27. Dhanani, J.; Fraser, J.F.; Chan, H.K.; Rello, J.; Cohen, J.; Roberts, J.A. Fundamentals of aerosol therapy in critical care. *Crit. Care* **2016**, *20*, 1–16, doi:10.1186/s13054-016-1448-5.
28. Lu, Q.; Girardi, C.; Zhang, M.; Bouhemad, B.; Louchahi, K.; Petitjean, O.; Wallet, F.; Becquemin, M.H.; Le Naour, G.; Marquette, C.H.; et al. Nebulized and intravenous colistin in experimental pneumonia caused by Pseudomonas aeruginosa. *Intensive Care Med.* **2010**, *36*, 1147–1155, doi:10.1007/s00134-010-1879-4.
29. WHO *Silver in drinking-water: Background document for development of WHO Guidelines for Drinking-water Quality*; Geneva, 2003;

30. Fewtrell, L. *Silver: Water disinfection and toxicity*; 2014;
31. Song, K.S.; Sung, J.H.; Ji, J.H.; Lee, J.H.; Lee, J.S.; Ryu, H.R.; Lee, J.K.; Chung, Y.H.; Park, H.M.; Shin, B.S.; et al. Recovery from silver-nanoparticle-exposure-induced lung inflammation and lung function changes in Sprague Dawley rats. *Nanotoxicology* **2013**, *7*, 169–180, doi:10.3109/17435390.2011.648223.
32. Stebounova, L. V.; Adamcakova-Dodd, A.; Kim, J.S.; Park, H.; O'Shaughnessy, P.T.; Grassian, V.H.; Thorne, P.S. Nanosilver induces minimal lung toxicity or inflammation in a subacute murine inhalation model. *Part. Fibre Toxicol.* **2011**, *8*, 5, doi:10.1186/1743-8977-8-5.